Cold/menthol TRPM8 receptors initiate the cold-shock response and protect germ cells from cold-shock–induced oxidation

Anne-sophie Borowiec, Benoit Sion, Fréric Chalmel, Antoine Rolland, Loïc Lemonnier, Tatiana de Clerck, Alexandre Bokhobza, Sandra Derouiche, Etienne Dewailly, Christian Slomianny, et al.

THE FASEB JOURNAL • RESEARCH • www.fasebj.org

Cold/menthol TRPM8 receptors initiate the cold-shock response and protect germ cells from cold-shock–induced oxidation

Anne-Sophie Borowiec,* Benoit Sion,† Frédéric Chalmel,‡ Antoine D. Rolland,‡ Loïc Lemonnier,* Tatiana De Clerck,* Alexandre Bokhobza,* Sandra Derouiche,* Etienne Dewailly,* Christian Slomianny,* Claire Mauduit,§ Mohamed Benahmed,§ Morad Roudbaraki,* Bernard Jégou,‡ Natalia Prevarskaya,* and Gabriel Bidaux*,¶,1

*Physiologie Cellulaire (PHYCEL), INSERM, U1003, Université Lille, Lille, France; †Pharmacologie Fondamentale et Clinique de la Douleur, INSERM, U1107, Neuro-Dol, Clermont Université, Université d'Auvergne, Clermont-Ferrand, France; ‡INSERM, U1085-Irset, Campus de Beaulieu, Rennes, France; §Centre Méditerranéen de Médecine Moléculaire (C3M), Team 5, INSERM, U1065, Nice, France; and, ¶Laboratoire de Physique des Lasers, Atomes et Molécules (PhLAM), UMR8523, Biophotonic Team, Villeneuve d'Ascq, France

ABSTRACT: Testes of most male mammals present the particularity of being externalized from the body and are consequently slightly cooler than core body temperature (4–8°C below). Although, hypothermia of the testis is known to increase germ cells apoptosis, little is known about the underlying molecular mechanisms, including cold sensors, transduction pathways, and apoptosis triggers. In this study, using a functional knockout mouse model of the cold and menthol receptors, dubbed transient receptor potential melastatine 8 (TRPM8) channels, we found that TRPM8 initiated the cold-shock response by differentially modulating cold- and heat-shock proteins. Besides, apoptosis of germ cells increased in proportion to the cooling level in control mice but was independent of temperature in knockout mice. We also observed that the rate of germ cell death correlated positively with the reactive oxygen species level and negatively with the expression of the detoxifying enzymes. This result suggests that the TRPM8 sensor is a key determinant of germ cell fate under hypothermic stimulation.—Borowiec, A.-S., Sion, B., Chalmel, F., Rolland, A. D., Lemonnier, L., De Clerck, T., Bokhobza, A., Derouiche, S., Dewailly, E., Slomianny, C., Mauduit, C., Benahmed, M., Roudbaraki, M., Jégou, B., Prevarskaya, N., Bidaux, G. Cold/menthol TRPM8 receptors initiate the cold-shock response and protect germ cells from cold-shock–induced oxidation. FASEB J. 30, 3155–3170 (2016). www.fasebj.org

KEY WORDS: hypothermia · spermatogenesis · apoptosis

In male mammals the mean testis temperature is ~4–8°C below the core body temperature. Internalization of testes in cryptorchidism and mild heating of testes, as well, have been reported to damage DNA and trigger apoptosis of germ cells leading to infertility (1). Testis cooling triggers similar effects. Indeed, testis hypothermia has been reported to increase germ cell apoptosis in both adult rats (2–4) and red-bellied newts (5). Concomitant to cell death, authors have described an increase in abnormal spermatozoa, a slight decrease in fertility, and a strong decrease in viable embryos. Among all germ cells, pachytene spermatocytes at stages XII–I were the most sensitive to cooling. These studies emphasize the thermosensitivity of gametogenesis and suggest that specific molecular protective pathways could intervene to control cell viability under mild temperature variations. Because hyperthermia is related to human disease, it has been extensively studied, whereas testes hypothermia has been described only on a macroscopic scale. Studying cold transduction

ABBREVIATIONS: CDKN, cyclin-dependent kinase inhibitor; CIRBP, cold-induced RNA-binding protein; CTDNEP1, CTD nuclear envelope phosphatase 1; CTL, control; ER, endoplasmic reticulum; FCS, fetal calf serum; GAPDH, glyceraldheyde-3-phosphate dehydrogenase; GDI2, GDP dissociation inhibitor 2; GPX, glutathione peroxidase; HSF, heat shock factor; HSP, heat shock protein; KO, knockout; KOM8, TRPM8-knockout; Magea, melanoma antigen family A; MKI67, monoclonal antibody Ki 67; mTOR, mammalian target of rapamycin; PCNA, proliferating cell nuclear antigen; Prm2, protamine 2; RBM3, RNA-binding motif protein 3; ROS, reactive oxygen species; SOD, superoxide dismutase; Tnp, transition protein; TRPM8, transient receptor potential melastatine 8; UCP, uncoupling protein

[1] Correspondence: CarMeN Laboratory, IHU Opera, INSERM U1060, Groupement Hospitalier EST, Bâtiment B13, 59 boulevard Pinel, F-69500 Bron, France. E-mail: gabriel.bidaux@univ-lyon1.fr

doi: 10.1096/fj.201600257R
This article includes supplemental data. Please visit *http://www.fasebj.org* to obtain this information.

mechanisms and molecular pathways leading to germ cell death may therefore give new insight into infertility but also into cold-protective strategy for other organs.

The cold- and menthol-activated transient receptor potential melastatine 8 (TRPM8) channel has been reported to be a thermodynamic sensor that detects cool temperatures in the range of 15–33°C (6, 7). In addition to its expression in dorsal root ganglia neurons and inner tissues, such as prostate (8), the TRPM8 channel is expressed in keratinocytes (9), where it regulates cold-dependent epidermal homeostasis (10, 11). Recent advances in the molecular mechanisms induced by TRPM8 activation have revealed that its cold transducer activity is tightly coupled to the level of reactive oxygen species (ROS) (10, 12, 13). In spermatozoa, low ROS levels facilitate capacitation, whereas at higher concentrations, they trigger tissue injury through cell death (14, 15). Based on the knowledge that TRPM8 is expressed in spermatozoa (16–18) and that ROS are well-known inducers of cell death, our goal in the current study was to understand whether the cold transducer, TRPM8, could trigger hypothermia-mediated apoptosis of male germ cells.

In this study, we demonstrate that the *Trpm8* gene is mostly expressed in pachytene spermatocytes and spermatids in which cold stimulation of rodent germ cells triggers calcium mobilization from internal stores. By means of a functional knockout (KO) of TRPM8 channels in mice, we showed that, loss of TRPM8 correlates with a temperature-independent increased level of germ cell death and with variation in the type of spermatozoa abnormality. We also report that suppression of TRPM8 decreased the viability of control (CTL; 29°C) and cooled (17°C) germ cells, but did not protect them from cold-induced apoptosis at 4°C. This inferred protective effect of TRPM8 expression in wild-type mice is related to a concomitant overexpression of antioxidant enzymes—namely, superoxide dismutase (SOD)-1; glutathione peroxidase-(GPX)-2, -4, and -5; and uncoupling protein 3 (UCP3). This TRPM8-dependent induction of protective factors correlates with a tight control of ROS concentration absent in TRPM8-KO (KOM8) germ cells.

In summary, we showed that TRPM8 channels are essential for the protection of germ cells against testis hypothermia, *via* a tight control of cell ROS concentration and induction of chaperons.

MATERIALS AND METHODS

Cell culture

The HEK cell line was purchased from the American Type Culture Collection (ATCC; Manassas, VA, USA). Cells were amplified in DMEM (Thermo Fisher Scientific Life Sciences, Courtaboeuf, France) supplemented with 10% fetal calf serum (FCS) and kanamycin (100 μg/ml). Cells were tested for contamination every 2 mo.

Establishment of *Trpm8*$^{-/-}$ mice

A complete description of the establishment of the *Trpm8*$^{-/-}$ mouse has been published (10). To suppress ion channel activity of every channel-like TRPM8 isoforms, introns 17 and 20 were deleted. Scale-up of *Trpm8*$^{-/-}$ colonies was achieved by backcrossing the *Trpm8*$^{-/-}$ line with the CTL *Trpm8*$^{+/+}$ line. According to the recommendations of The Jackson Laboratory (Bar Harbor, ME, USA; *https//:www.jax.org*) for breeding strategies, interbreeding was performed for 8 generations to prevent substrain apparition and genetic divergence. At the time of the experiments, CTL mice were aged 78 wk and KOM8 mice 68 wk, on average. The mice were distributed randomly in each temperature groups by rolling dice.

Cold shock of mouse testes

Heat-treated mice were anesthetized with an injection of 10 mg/kg xylazine and 100 mg/kg i.p. ketamine. After anesthesia, the scrotum of each male was passed through a hole that was then placed in a circulating water bath at 0 or 14°C for 45 min. To calibrate cooling speed and efficiency, we measured evolution of the core and scrotum temperatures. To measure the former temperature, an incision was made in the abdomen, and the probe of a digital thermometer Digitron (Digitron, Devon, UK) was inserted into the abdominal cavity. The probe was pushed down into the scrotum to measure its temperature. We measured core and scrotum temperature of mice partially immerged in cool (14°C) and cold (0°C) water for 45 min, whereas CTL animals received anesthesia only. A CTL experiment was performed at 29°C, which was found to be the temperature in the scrotum of anesthetized animals. This temperature is lower because of the combination of 2 factors: the effect of the anesthetic on body temperature and the testicular descent into the scrotum during anesthesia. As presented in Supplemental Fig. S1*D*, the scrotum temperature dropped and stabilized at 4–5°C within 10 min (rate of decrease, 6.2°C/min). By comparison, the rate of body temperature cooling was ~0.38°C/min (Supplemental Fig. S1*E*). After 45 min of immersion, mice were in severe hypothermia, preventing us from prolonging the experiment. (Under those experimental conditions, mice viability was 100% 3 days after immersion.) After waking up, all animals were returned to their cages. Mice from each group were killed by cervical dislocation, and their testes and epididymis were removed and weighed. Spermatozoa were prepared from minced epididymis after incubation in 3 ml of BWW with stirring during 15 min. An aliquot was diluted with a sodium acid carbonate-formaldehyde solution and placed into the chamber of a hemocytometer (Thomas Scientific, Inc., Swedesboro, NJ, USA). Spermatozoa were counted according to the techniques described by the World Health Organization (19). Sperm preparation smears were made and allowed to dry in air; 200 spermatozoa were examined at ×400 magnification.

Isolation and culture of germ cells

After the mice were killed, testes of C57BL/6J mice were collected. The tunica albuginea of the testes was removed. Tubules were then digested in F12/DMEM (1:1) containing 0.5 mg/ml collagenase at 32°C for 15 min under gentle agitation. Seminiferous tubules were harvested by low-speed centrifugation and washed twice with F12/DMEM without enzyme. The pellet was resuspended in F12/DMEM supplemented with antibiotics and containing 0.5 mg/ml collagenase and 10 μg/ml DNAse. Seminiferous tubules were then cut in fragments with 2 lancets and digested as described above. The dispersed seminiferous cords and cells were collected by centrifugation (1000 rpm, 8 min), washed, and gently resuspended in culture medium F12/DMEM supplemented with 5% FCS, MEM vitamin (1×), ITS liquid medium supplement (1×), sodium pyruvate (1 mM), and antibiotic/antimycotic. The

whole process was performed in conditions that limited thermal shocks.

Transfection

HEK cells were transfected with plasmids by using Nucleofector technology (Lonza Group Ltd., Basel, Switzerland) according to manufacturer. Cells (10^6) were transfected with 2 μg of total vectors and plated on dishes precoated with polylysine.

Microarray and RNA-seq datasets

To study *Trpm8* expression in mammalian testes, we made use of 3 published datasets, including transcriptomes of different types of male germ cells and of testicular somatic cells (20–22). We first used a transcriptomic dataset based on Affymetrix 3′ IVT microarrays including 4 testicular cell types in 3 mammalian species (human, mouse, and rat) (ArrayExpress ID: ETABM-130; Thermo Fisher Scientific) (20): Sertoli cells (only for mouse and rat), spermatogonia (only mouse and rat), spermatocytes, round spermatids, and total testis. Log_2-transformed normalized expression patterns of *Trpm8* transcript were then plotted in all 3 species, using the corresponding probe sets: 1369348_at, 1421617_at, and 1369348_at in rat, mouse, and human, respectively (**Fig. 1*A***). Finally, expression patterns of *Trpm8* based on RNA sequencing data, as published by Gan *et al.* (21), Soumillon *et al.* (22), and Darde *et al*. (23) were examined in the ReproGenomics Viewer (21–23) (Fig. 1*B*).

Invariant gene selection for qPCR normalization

Invariant genes were selected from high-throughput microarray experiments on mouse postnatal testis development and mouse isolated testicular cells (20, 24–26). Corresponding datasets were downloaded from the Gene Expression Omnibus (GEO) repository (National Center for Biotechnology Information, Bethesda, MD, USA; *http://www.ncbi.nlm.nih.gov/geo/*) and normalized by using the RMA algorithm (27) in AMEN software (28). Probesets that were significantly detected (*i.e.*, signal intensity > median value of all probesets) and showed a low signal variation across all samples (*i.e.*, SD of log2-transformed intensity < 0.2) were selected. Expression profiles for candidate genes were finally individually checked at the GermOnline website [http://www.germonline.org/index.html (29)]. Final selection included GDP dissociation inhibitor 2 (Gdi2; probeset 1435898_x_at), CTD nuclear envelope phosphatase 1 (Ctdnep1; probeset 1452100_at), and glyceraldheyde-3-phosphate dehydrogenase (Gapdh; probeset 1418626_s_at) (Supplemental Fig. S3).

PCR

A classic RT-PCR protocol was used, as described elsewhere (30). Oligonucleotides are presented in **Table 1**.

Quantitative real-time PCR analysis

Real-time quantitative PCR was performed as has been described (10). Primer sequences are given in Table 1. In the case of tissue analysis and multiple biological variables, proper selection of reference genes cannot be achieved randomly. Therefore, after microarray analysis, we selected 3 genes (*Gapdh*, *Gdi2*, and *Ctdnep1*) expressed in different subtypes of germ cells and in different cell types constituting testis tissue, as well, which showed the most stable expression (Supplemental Fig. S3*A*). We checked the stability of expression of the reference genes in CTL and KOM8 testis that had been subjected or not to mild and strong hypothermia (Supplemental Fig. S3*B*, *C*). Because we detected minor asymmetric variations, we concluded that the 3 reference genes should be used for normalization instead of arbitrarily selecting 1 or 2 of them. C_t,ref was replaced with a normalization factor, C_q, calculated by geometric averaging of the C_t of the 3 reference genes (31). Scatterplots of *Gapdh*, *Gdi2*, and *Ctdnep1* C_t values in function of C_q revealed a better correction of gene expression (Supplemental Fig. S3*D*).

Immunoblot analysis

Tissues were collected and stored in liquid nitrogen until protein extraction. Pieces of testes were transferred in beads-containing tubes and extracted with a high-throughput Precellys-24 tissue homogenizer (Precellys, Saint-Quentin-en-Yvelines, France) cooled down with Cryolis (Activair, Opava, Czech Republic) at 4°C. Cultured cells were collected in a PBS solution and then pelleted before extraction in the ice-cold buffer. Proteins were extracted, and immunoblot analysis was performed (10). Total protein (25 μg) was loaded onto a polyacrylamide gel (100 μg for TRPM8 detection). The membrane was blocked in TNT [15 mM Tris buffer, pH 8, 140 mM NaCl, and 0.05% Tween 20+5% (w/v) nonfat dry milk] for 30 min at room temperature and then soaked in primary antibody diluted in TNT+1% milk for 2 h at room temperature. After 3 washes, the membrane was soaked in secondary antibody diluted in TNT+1% milk for 1 h at room temperature. It was processed for chemiluminescence detection with Luminata Forte Western HRP Substrate (Millipore, Guyancourt, France). After a 10 min bath in Reblot Plus Mild Solution (Millipore), the immunoblot analysis was performed again. The primary antibodies were as follows: TRPM8, 1:1000 (ab109308; Abcam); heat shock protein A1 (HSPA1), 1:500 (sc-1060; Santa Cruz Biotechnology, Dallas, TX, USA); HSPA2, 1:2000 (ab83204; Abcam, Cambridge, United Kingdom); heat shock factor 1-C5 (HSF1-C5), 1:500 (sc-17756; Santa Cruz Biotechnology); HSF2, 1:500 (sc-13056; Santa-Cruz); CIRP, 1:200 (sc-161012; Santa Cruz Biotechnology); monoclonal antibody Ki 67 (MKI67), 1:500 (Ab15580; Abcam); SOD1, 1:500 (sc-11407; Santa Cruz Biotechnology); SOD2, 1:500 (sc-133254; Santa Cruz Biotechnology); GPx4, 1:200 (sc-50497; Santa-Cruz); GPx5, 1:200 (sc-54826; Santa-Cruz Biotechnology); β-actin, 1:1000 (A-2228; Sigma-Aldrich); protamine 2 (Prm2) 1:200 (sc-23102; Santa-Cruz Biotechnology); phospho-mammalian target of rapamycin (p-MTOR) (Ser^{2448}), 1:200 (sc-101738; Santa-Cruz Biotechnology); and mTOR, 1:200 (sc-8319; Santa-Cruz Biotechnology).

Histology

Deparaffinized slides of testis from 8 $Trpm8^{+/+}$ and 8 $Trpm8^{-/-}$ mice were subjected to hemalum-erythrosin-safran trichrome staining. The slides were analyzed on an upright Axio Imager.A1 microscope (Zeiss, Oberkochen, Germany). Images were acquired with an AxioCam MRc5 digital camera, and the Axiovision software (Zeiss) was used for analysis.

Immunohistofluorescence

After paraffin removal, antigen retrieval was achieved in a citrate buffer boiled 4 times for 5 min in a microwave oven. After 3 washes in PBS, the tissue sections were blocked with PBS supplemented with 1.2% gelatin (PBS/gelatin) for

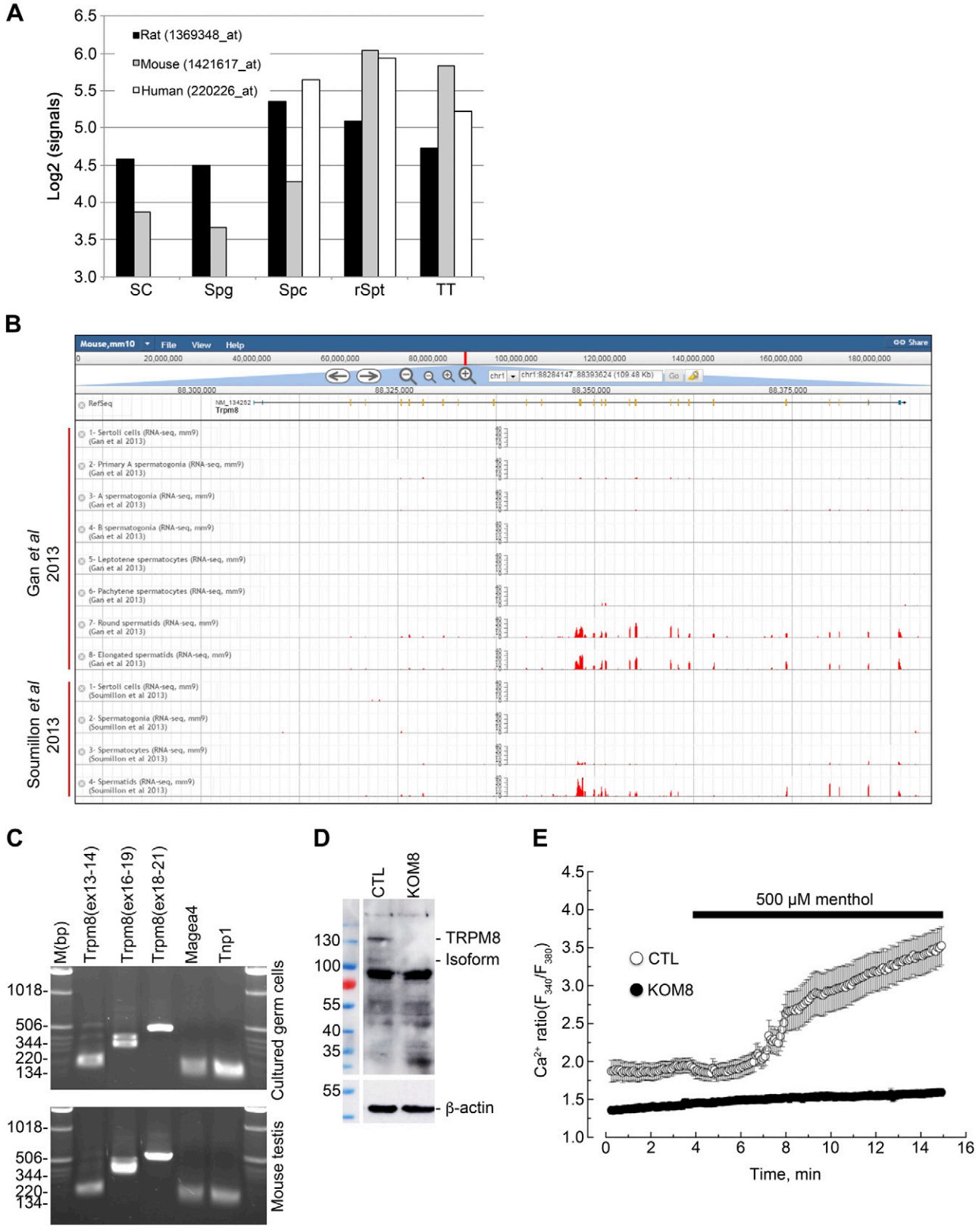

Figure 1. TRPM8 channels are expressed and functional in mouse germ cells. *A*) Normalized signal intensities (*y* axis, log2-transformed) of *Trpm8* are shown in the different testicular cell types (*x* axis) in Sertoli cells (SC), spermatogonia (Spg), spermatocytes (Spc), round spermatids (rSpt), and total testis (TT) of 3 mammalian species: rat, mouse, and human. *B*) Gene structure is shown for *Trpm8* and histograms of the numbers of RNA-seq reads that aligned the corresponding genomic locations across the different samples from Gan *et al.* (21) and Soumillon *et al.* (22) (*y*-axis ranges from 0 to 40) (adapted from The ReproGenomics Viewer; *http://rgv.genouest.org/publication.html*). *C*) PCR detection of different regions of Trpm8 in cultured germ

(*continued on next page*)

TABLE 1. *Primers*

Gene	Forward (5–3′)	Reverse (5′–3′)
PCR		
Trpm8(ex13–14)	TGAAGCTTCTGCTGGAGTGG	GAGTTCCACATCCAAGTCCTC
Trpm8 (ex16–19)	ATATGAGACCCGAGCAGTGG	CTGCCTCACTTCATCACAGAAG
Trpm8 (ex18–21)	CGAGACACGAAGAACTGGAAG	ATCCGTTGCAGAATTATAATCTGGG
Trpm8 (ex16–21)	ATATGAGACCCGAGCAGTGG	ATCCGTTGCAGAATTATAATCTGGG
β-Actin	CAGAGCAAGAGAGGTATCCT	GTTGAAGGTCTCAAACATGATC
Real-time PCR		
Gapdh	CTGCGACTTCAACAGCAACTC	TCCACCACCCTGTTGCTGTA
Gdi2	GGAATACGACGTGATCGTGC	CAGCGGTGTTATAGACGCACT
Ctdnep1	ACAAACACCCAGTCCGGTTT	TGCCACAGCAGAGCCATAAA
Trpm8	CACATATGACTTCTCCCACTGT	AGAGCATGTAGATGCACACCA
Magea4	GGGAGTTAGACAATGTTCAGGCT	GGAGAGGAGGCTCTTTGAGG
Hspa2 (variant 1)	CGCTTTCGTCCTAACGTTGC	CGATGATCTCCACCTTGCCA
Tnp1	CTCACAAGGGCGTCAAGAGA	CATTGCCGCATCACAAGTGG
Prm2	CATAGGATCCACAAGAGGCG	TGCCTCCTACATTTCCTGCAC
Mki67	TCTTGGCACTCACAGCCCAGC	TGTCCTCGGTGGCGTTATCCC
Pcna	TCTGCAAGTGGAGAGCTTGGCA	AGAGCAAACGTTAGGTGAACAGGCT
Cdkn1a	CGGTGTCAGAGTCTAGGGGA	AGGATTGGACATGGTGCCTG
Cdkn1b	GCTGGGTTAGCGGAGCAGTGT	AGCGTTCGGGGAACCGTCTG
Mtor	GCATTCCGACCGTCCGCCTT	CTGGAACGCCGCAGTCCGTT
Sp1	GTGCCGCCTTTTCTCAGACT	CAATTCTGCTGCAGGTTGCT
Ddit3	TGCAGGAGGTCCTGTCCTCAGAT	AGCCAAGCTAGGGACGCAGG
Atf4	CATGGGTTCTCCAGCGACAA	TCCAACATCCAATCTGTCCCG
Eif2ak3	CAAGCCAGAGGTGTTTGGGA	AGATTCGAGCAGGGACTCCA
SigmaR1	AGGGCACCACGAAAAGTGAGGT	GGTCCCCACTCCAGAGCCGT
Hsf1	GCCTCCCCAGGCAGGAGCATA	AGGGCTCGCCTCCAGTACCC
Hsf2	CATCACCTGGAGTCAGAATGGA	GCACTACTTTTCGGAAGCCA
Cirbp	GGAGCTCGGGAGGGTCCTACA	GACGATCTGGACGCGGAGGG
Hspa1a	TGGCCTTGAGGACTGTCATT	AGCCCACGTGCAATACACAA
Rbm3	CGTGGTCGCAGTTACTCTAG	TGAGTAGCGGTCATAGCCAC
Ucp1	AGGAGTCCGAAGTCGCGGGT	TGGAGGGCAGAGAGGCGTGA
Ucp2	TCTGCACCACCGTCATCGCC	GACCTGCGCTGTGGTACTGGC
Ucp3	CCGAAGTGCCTCCCACAACGG	ACGGACCTTGGCGGTGTCCA
Sod1	GCGGTGAACCAGTTGTGTTG	GCACTGGTACAGCCTTGTGT
Sod2	ACAACTCAGGTCGCTCTTCAG	TCCAGCAACTCTCCTTTGGG
Sod3	CTGACAGGTGCAGAGAACCTC	GGTCAAGCCTGTCTGCTAGG
Cat	GCCAATGGCAATTACCCGTC	GAGGCCAAACCTTGGTCAGA
Gpx1	TCTCTCTGAGGCACCACGAT	CATTCTCCTGGTGTCCGAACT
Gpx2	CTGCAATGTCGCTTTCCCAG	CCCCAGGTCGGACATACTTG
Gpx3	GCATCCTGCCTTCTGTCCC	CGATGGTGAGGGCTCCATAC
Gpx4	GTACTGCAACAGCTCCGAGT	ATGCACACGAAACCCCTGTA
Gpx5	TGTGAAAGGCACCATCTACG	GACCGCAATAGGTAGCCACA

30 min at 37°C and then coincubated with primary antibodies diluted in PBS/gelatin for 2 h at 37°C. After thorough rinsing in PBS/gelatin, the slides/dishes were treated with the corresponding secondary antibody: either Dye light 488-labeled anti-rabbit IgG (1:2000) or Texas Red-labeled anti-goat IgG (1:800; both from Jackson ImmunoResearch, West Grove, PA, USA) diluted in PBS/gelatin for 1 h at RT. After rinsing twice in PBS/gelatin and once in PBS with 1:200 DAPI for 10 min at room temperature, the slides were mounted with Mowiol (Sigma-Aldrich) and examined under an LSM 780 confocal microscope (Zeiss).

TUNEL was performed on deparaffinized slides of mouse testis, by means of TUNEL-TMR red (Roche, Meylan, France), incubated at room temperature for 30 min. After the slides were rinsed twice in PBS/gelatin and once in PBS with 1:200 DAPI for 10 min at ambient temperature, they were mounted with Mowiol. Images were acquired with an AxioCam MRc5 digital camera, and the Axiovision software was used for analysis (Zeiss). Because numerous meiotic cells are visible in testis slices and because they usually display an increased TUNEL signal related to DNA breaks occurring in meiosis, the slices were illuminated to discriminate the highest fluorescence

cells (top) and in whole extracts of mouse testis (bottom). PCR fragments were amplified from exon X to Y and reported as *Trpm8(exX-Y)*. Melanoma antigen family A-4 (*Magea 4*) and transition protein 1 (*Tnp1*) were used as reporters of spermatogonia and spermatids respectively. *D*) Immunoblot analysis reveals detection of full-length TRPM8 (130 kDa) and a 105 kDa TRPM8 isoform, as well, in total protein extract of CTL mouse testis, but not in TRPM8-KO (KOM8) mouse testis. *E*) Calcium imaging experiments realized with Fura2-AM fluorescent probe show an increased cytosolic Ca^{2+} concentration in 2 d isolated $Trpm8^{+/+}$ mouse germ cells (CTL; $n = 20$) after addition of 500 μM menthol. No Ca^{2+} variation was detected in germ cells of $Trpm8^{-/-}$ mouse line (KOM8; $n = 83$).

emission of apoptotic cells from the smallest fluorescence emission of meiotic cells.

Flow cytometry

ROS contents in freshly isolated mouse germ cells were measured by the mean of fluorescent reporters analyzed by a CyAn ADP flow cytometer (Beckman-Coulter, Brea, CA, USA). After the dissociation of mouse testis, germ cells were incubated concomitantly with 2.5 μM CellRox Deep Red reagent and 2.5 μM CellRox Green reagent for 45 min (CellRox; Thermo Fisher Scientific). After two 5 min washes, the cells were incubated for 1 h at 32, 20, or 8°C before flow cytometer analysis. Fluorescent reagents were excited specifically by means of 488 and 633 nm lines, and emission was filtered with a series of specific filters to avoid bleed through. The flow cytometer was calibrated with rainbow beads before each experiment. 405, 488, and 642 wavelength lasers were used according to fluorescent reporters. Data were analyzed with FlowJo software (ver. 8.7; TreeStar, Ashland, OR, USA).

Wide-field Ca^{2+} imaging

Calcium imaging experiments were performed (32). $[Ca^{2+}]_c$ was measured by using the ratiometric dye Fura-2 and was quantified according to the Grynkiewicz equation (33). The bath solution contained (in mM) 140 NaCl, 5 KCl, 2 $CaCl_2$, 2 $MgCl_2$, 0.3 Na_2HPO_4, 0.4 KH_2PO_4, 4 $NaHCO_3$, 5 glucose, and 10 HEPES; pH adjusted to 7.3 with NaOH; and osmolarity: 330 mOsm/L.

Electrophysiology

Membrane currents were recorded in the whole-cell configuration by using the patch-clamp technique and a computer-controlled EPC-9 amplifier (HEKA Elektronic, Lambrecht, Germany). Patch pipettes were made with a P-97 puller (Sutter Instrument, Novato, CA, USA) from borosilicate glass capillaries (WPI, Sarasota, FL, USA). Patch-pipettes (resistance, 3–5 MΩ) were filled with the following solution (in mM): 140 CsCl, 10 HEPES, 8 EGTA, 1 $MgCl_2$, and 4 $CaCl_2$ (100 nM free Ca^{2+}), pH 7.2 (adjusted with CsOH); osmolarity: 290 mOsm/L. The extracellular solution contained (in mM) 150 NaCl, 5 KCl, 10 HEPES, 10 glucose, 1 $MgCl_2$, and 2 $CaCl_2$ (pH 7.3; adjusted with NaOH); osmolarity: 310 mOsm/L.

Data analysis

Each experiment was repeated at least 3 times, and the results are expressed as means ± SD. The data were analyzed and graphs plotted using Origin 5.0 software (Microcal, Northampton, MA, USA). Prism (GraphPad Software Inc., San Diego, CA, USA) was used for statistical analysis. Statistical significance was set at $P < 0.05$, calculated by unpaired t test with Welch's correction and 1-way ANOVA with Tukey's multiple comparison posttest (≥3 groups). Alternatively, 1-way ANOVA with Tukey's multiple-comparison posttest (≥3 groups), statistical significance was assumed at $P < 0.05$; the number of the "CTL" column (shown at the bottom of each CTL histogram) is indicated on the top of the "tested" column in the histogram figures. For financial constraints and given that we sought to detect gene and protein variations greater than almost 2-fold, the size of the group was limited to 4, to obtain a size effect of 1 (low sensitivity), a statistical power of 0.8 (high specificity), and $\alpha < 0.05$ with 1-way ANOVA, assuming that σ of all groups was 1.

RESULTS

TRPM8 isoforms are expressed in meiotic germ cells in rodent testis

The profiling of *TRPM8* expression in different germ cell subtypes and in somatic cells was achieved by Affymetrix 3′ IVT microarrays and Illumina RNA sequencing (Illumina; San Diego, CA, USA) in 3 mammalian species (human, mouse, and rat) (20–22) (**Fig. 1*A*, *B***). We found a higher expression of *Trpm8* in both meiotic and postmeiotic germ cells than in the other cell types in all 3 species (Fig. 1*A*). Analysis of 2 RNA-sequencing datasets in the mouse unambiguously revealed an enrichment of the *Trpm8* region from exon 12 to 26 in postmeiotic germ cells (21, 22) (Fig. 1*B*). PCR amplifications confirmed the expression of *Trpm8* (Fig. 1*C*), including transmembrane and P-loop encoding exons (Supplemental Fig. S1*A*), in both mouse testis and 3-d primary culture of mouse germ cells. To inactivate all TRPM8 channel isoforms, we developed a functional KO mouse line, KOM8, by deleting exons 18, 19, and 20, which encode the active pore domain. Immunoblot analysis of TRPM8 protein performed on total testis extract showed the detection of the full-length TRPM8 and an ~105 kDa isoform (Fig. 1*D*). Video fluorimetry revealed that menthol application induced a calcium mobilization in primary cultures of germ cells isolated from $Trpm8^{+/+}$ CTL mice (Fig. 1*E*). Conversely, germ cells from $Trpm8^{-/-}$ KOM8 mice were characterized by an absence of $[Ca^{2+}]_i$ variation. Electrophysiological recordings failed to detect any TRPM8 currents in mouse germ cell plasma membranes (Supplemental Fig. S1*C*), whereas the positive controls in HEK cells transfected with full-length TRPM8 were characterized by the typical cold-activated current (8). These data suggest that functional TRPM8 channels located within the endoplasmic reticulum (ER) membrane participate in ER Ca^{2+} signaling in germ cells. Because TRPM8 proteins incorporate a cold sensor in their C terminus (34), we wondered whether TRPM8 channels could participate in testis response to hypothermia.

TRPM8 suppression sensitizes mouse germ cells to apoptosis

Hypothermia of mouse scrotum was obtained by immersion of the scrotum. This protocol offers the advantage of rapid cooling of testis tissue while limiting core hypothermia, thus increasing overall survival. As expected, when the cold sensor, with an activation range spanning from 15 to 32°C, was inactivated, the KOM8 mice showed a defect of adaptive thermogenesis resulting in rapidly developing hypothermia in the mild cold condition. Indeed, cooling the testes at 17°C for 45 min reduced the core body temperature of the KOM8 mice to 22.1 ± 0.8°C, a value significantly lower than the 25.6 ± 1.5°C recorded in wild-type animals (**Fig. 2*A***). This differential amplitude of hypothermia was attenuated when the temperature was held at 4°C. This result suggests that TRPM8-stimulated thermogenesis cannot attenuate strong cold-induced hypothermia. After a 3 d recovery

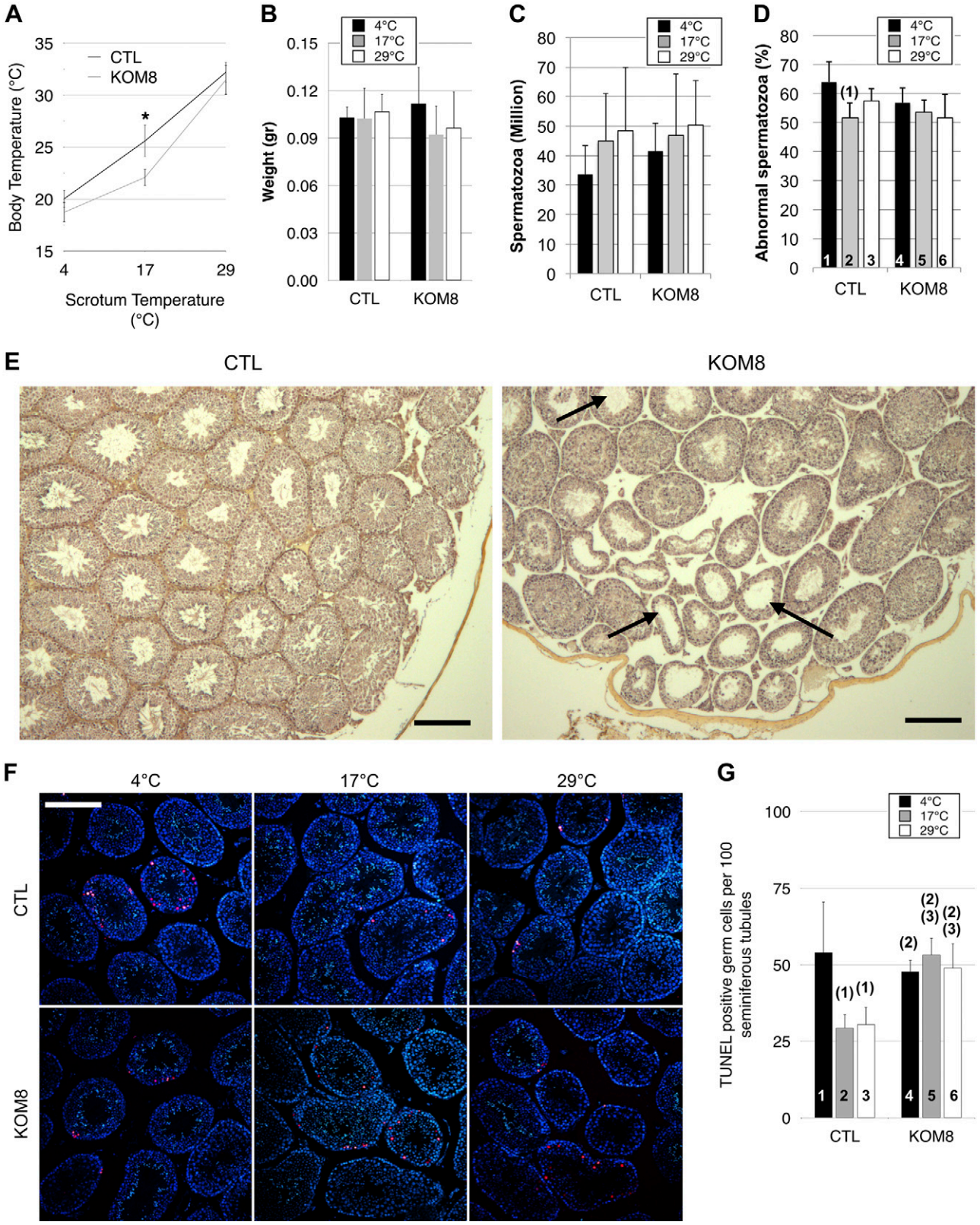

Figure 2. TRPM8 channel expression protects germ cells from apoptosis at rest and during mild, but not noxious, cold exposure. *A*) *Trpm8*$^{+/+}$ (CTL) and *Trpm8*$^{-/-}$ (KOM8) mice were subjected to a 45 min cold shock, and both body and scrotum temperatures were measured concomitantly. Mild cold (17°C) revealed an impaired thermogenesis of KOM8 testis, whereas no alteration appeared under noxious cold conditions (4°C). *B–D*) Testicular weight (*B*), spermatozoa concentration (*C*), and percentage of abnormal spermatozoa (*D*) in CTL and KOM8 mouse testes subjected to cold shocks of different magnitudes did not show any significant difference 3 d after treatment. Statistical significance was assumed when $P < 0.05$ and is shown above the tested column as the number of the column it is paired to. *E*) Anatomopathological analysis revealed the presence of near-empty

(*continued on next page*)

period, the mice were euthanized and the testes collected. No difference in testis weight (Fig. 2*B*), spermatozoa count (Fig. 2*C*), or percentage of abnormal spermatozoa (Fig. 2*D*) were detected between KOM8 and CTL mice after the 3 d recovery period. Nevertheless, differences in the distribution of the type of abnormal morphology were determined (Supplemental Fig. S2). Histologic analysis revealed a significantly higher number of empty seminiferous tubules in KOM8 testis of mice housed at an ambient temperature (Fig. 2*E*). In line with these studies of rat and newt (2, 3, 5), apoptosis of CTL germ cells was doubled by cold exposure (Fig. 2*F*, *G*). KOM8 germ cells exhibited a cold-independent apoptotic population with a basal apoptosis level similar to the one recorded in CTL cells at 4°C. These results suggest that, in wild-type mice, TRPM8 channels protected germ cells exposed to mild cold (17–29°C) against apoptosis. This latter range of temperature correlates with the window of TRPM8 activation by cold (35, 36). To decipher how TRPM8 protects germ cells against cold-induced cell death, we looked for potential deregulation of gene families in germ cells of CTL mice subjected to hypothermia.

Hypothermia exerts a TRPM8-dependent regulation of gene expression in testis

Using qPCR, we specifically screened the expression of genes involved in the cell cycle, mitochondrial uncoupling, oxidation, and genes activated by cold. To avoid false-positive variations in gene expression, we first carefully defined a normalizing factor as described in Materials and Methods. This factor was selected among the most invariant genes detected in CTL and KOM8 testes subjected or not to hypothermia (Supplemental Fig. S3). We first checked whether cold could have modified the rate of gametogenesis and unbalanced the proportion between germ cell subtypes, but significant variation of marker expression was detected in KOM8 and CTL testes after a 3 d recovery period (Supplemental Fig. S4). Based on these observations, we then assumed that any variation in gene expression detected in the following experiments would solely result from a true shift in the transcription rate and not from major changes in cell population heterogeneity. We then controlled to ensure that the level of TRPM8 transcripts was stable in both KOM8 and CTL testis, independent of the incubation temperature, by quantifying the expression of exons 21 to 22 downstream of the deleted region in KOM8 (**Fig. 3*A***). In addition to dedicated proteins, HSPs are also regulated by cold shock (37, 38). We found a weak induction of *Hsf1*, cold-induced RNA-binding protein (*Cirbp*), and RNA-binding motif protein 3 (*Rbm3*) in CTL testis subjected to strong hypothermia (4°C). This cold-mediated gene induction was suppressed in KOM8 testis (Fig. 3*B*). This result suggests a TRPM8- and cold-dependent up-regulation of these genes. Conversely, the expression of the HSP-70 gene *Hspa1a* was decreased during cold induction in CTL mouse testis but remained unchanged in KOM8 mouse testis (**Fig. 4**). The cell cycle markers Ki67 (*MKi67*), proliferating cell nuclear antigen (*PCNA*), and $p27^{kip1}$ [cyclin-dependent kinase inhibitor 1B (*Cdkn1B*)] were not affected by cold, whereas $p21^{cip1}$ (*Cdkn1A*), involved in cell cycle arrest, was preferentially induced by the cold in KOM8 testis (Fig. 3*C*). Because TRPM8 has been implicated in modifications of ROS homeostasis (13) and because elevated ROS concentration could induce an increased apoptosis of germ cells paired with modifications in spermatozoa phenotype and survival (39), we measured the expression level of genes coding for the detoxifying enzymes SOD1 and -2 (*Sod1* and *Sod2*), GPX1–5 (*Gpx1–5*), and catalase. Because uncoupling protein (UCP) 3 (*Ucp3*) has been reported to participate in ROS homeostasis (40), we also measured the expression of *Ucp3*. As shown in Figs. 3D and 4, *Sod1*, *Gpx2*, *Gpx5*, and *Ucp3* were induced by cold in CTL testis, but not in that of the KOM8s. Surprisingly, mild cold (17°C) induction of the testis-specific peroxidase *Gpx4* was restricted to CTL mice, although intense cold (4°C) induced the *Gpx4* gene in both CTL and KOM8 mouse testes (Fig. 3*D*). We finally tested for genes involved in the ER stress response and cell signaling, but no significant variations were detected (Fig. 4). These results, altogether, indicate that cold (4°C) induction of *Hsf1*, *Cirbp*, *Rbm3*, *Sod1*, *Gpx2*, *Gpx5*, and *Ucp3* genes and cold repression of the *Hspa1a* gene requires TRPM8 channels (**Table 2**). It should be noted that the highest *Gpx4* induction is reached with mild cold (17°C) stimulation.

Immunoblot analysis partially confirmed the above results for HSPA1, SOD1, GPX4, and GPX5 proteins in extracts of mouse testis 3 d after hypothermia. Note that, although its expression was unchanged at the mRNA level, we observed a down-regulation of HSPA2 protein in CTL testis subjected to hypothermia and in KOM8 mice at 29°C (**Fig. 5*A*, *B***), suggesting a cold-dependent post-transcriptional regulation of HSPA2 protein. Immunolabeling of CTL mouse testis slices confirmed this decrease in HSPA2 expression after hypothermia, whereas CIRBP appeared stable (Fig. 5*C*). In the same line of evidence, KOM8 mice showed a decreased level of CIRBP expression (Fig. 5*D*), confirming that variations in immunoblot results were mostly related to decrease in expression per cell, instead of a decreased proportion of cell population in testis. It has recently been shown that cold shock inhibits mTOR (41). Although *mTor* expression was unchanged at the mRNA level (**Fig. 4**; Table 2), the level of phosphorylation of mTOR showed a tendency to decrease with cold shock (Fig. 5*A*). This finding may suggest that TRPM8 participates in the upstream regulation of mTOR inhibition.

seminiferous tubules (arrows) in trichromatic-stained paraffin-embedded sections of KOM8 testis of nonstimulated mice. Scale bars, 200 μm. *F*) TUNEL with nucleotides coupled to tetramethyl rhodamine (red) revealed apoptotic germ cells. Nuclei were counterstained with DAPI (blue). Apoptotic cells were counted and normalized by 100 seminiferous tubules. Scale bar, 200 μm. *G*) Histogram shows statistical analysis of the counting of apoptotic germ cells. Values are means ± SD for CTL ($n = 6$) and KOM8 ($n = 6$) mice. Statistical analysis was performed by 1-way ANOVA.

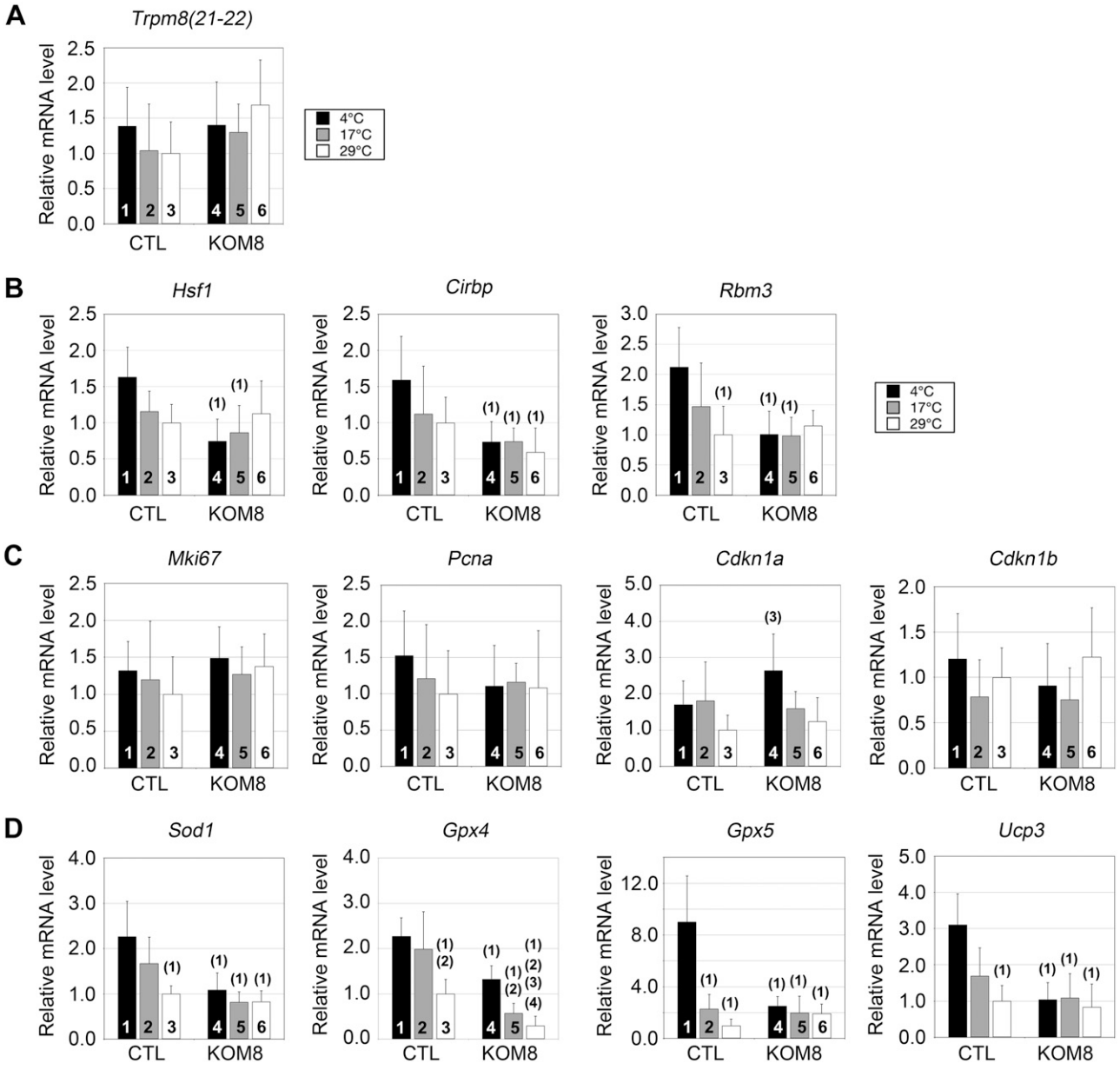

Figure 3. Screening of specific gene networks reveals the TRPM8-dependence of genes encoding cold-shock proteins and antioxidant enzymes. *A*) Real-time PCR showed no significant variation in *Trpm8* gene expression (exons 21–22) in CTL and KOM8 mice subjected to cold shocks of different amplitudes (scrotum temperatures were 29, 17, and 4°C). *B–D*) mRNA quantification was also performed for the following heat- and cold-shock factors (*B*): heat-shock factor 1 (*Hsf1*), cold-inducible RNA binding protein (*Cirbp*) and RNA binding motif (RNP1, RRM) protein 3 (*Rbm3*); for proliferation markers (*C*): antigen identified by monoclonal antibody Ki 67 (*Mki67*) and proliferating cell nuclear antigen (*Pcna*); inhibitors of cell cycle: cyclin-dependent kinase inhibitor 1A and 1B (*Cdkn1a* and *Cdkn1b*, respectively) also known as $p21^{cip1/waf1}$ and $p27^{kip}$; and for antioxidant enzymes (*D*): SOD1, Cu^{2+}/Zn^{2+} (*Sod1*, *Gpx4*, and *Gpx5*, respectively) and UCP3 (*Ucp3*). Values are presented as means ± SD for CTL ($n = 5$) and KOM8 ($n = 5$) mice. Statistical significance confirmed with 1-way ANOVA when $P < 0.05$ and is indicated above the tested column as the number of the CTL column it is paired to.

Although testis responses to hypothermia were measured 3 d after cold shock, the observed gene deregulation represented long-term responses after kinetic apoptosis. Induction of detoxifying enzymes suggests that cold shock is concomitant with a boost in [ROS], which would explain the induction of apoptosis found in the present study. However, since we analyzed whole testis tissue, we could not clearly state that the observed gene regulations occurred in germ cells instead of in spermatozoa or any testicular somatic cells. This result is of primordial interest because cold-induced apoptosis was restricted to germ cells. Because of the dense vasculature of testis and the thermogenesis activated by the cold shock, it is unlikely that the core testis temperature dropped along with the scrotal temperature. To compare the results of hypothermia performed on testis of live animals with hypothermia performed on isolated germ cells, we assumed that cold shocks on the latter would be better performed several degrees above the temperatures applied on animals. We thus studied the response of isolated germ cells to mild and

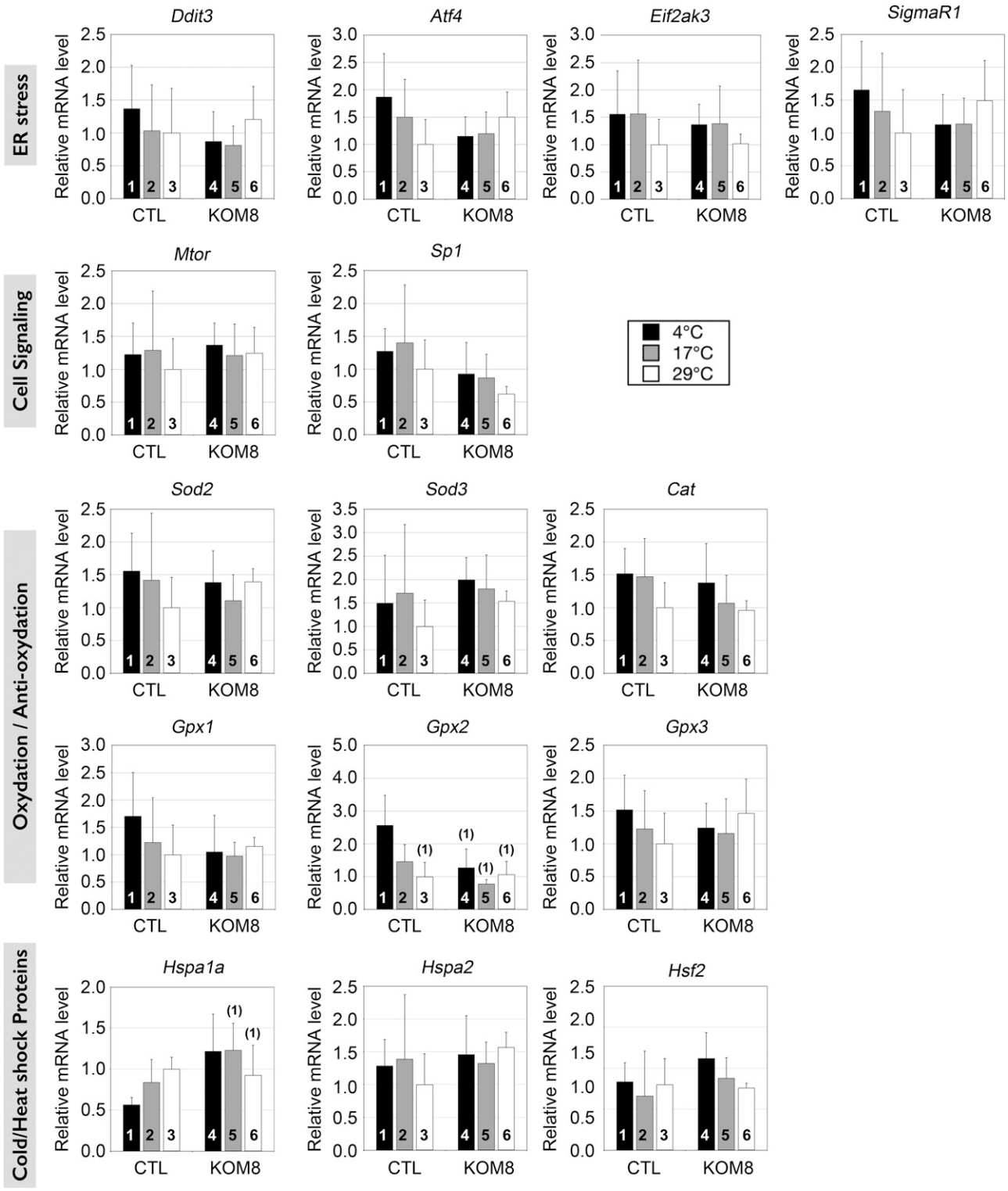

Figure 4. Real-time PCR screening of several genes families in mouse testis 3 d after cold shocks. As in Fig. 3, graphs show real-time PCR quantification of gene expression of ER stress marker: DNA-damage-inducible transcript 3 (*Ddit3*), activating transcription factor 4 (*Atf4*), eukaryotic translation initiation factor 2-α kinase 3 (*Eif2ak3*), σ nonopioid intracellular receptor 1 (*Sigmar1*); cell signaling markers: mechanistic target of rapamycin (serine/threonine kinase) (*Mtor*) and Sp1 transcription factor (*Sp1*); oxidation/anti-oxidation enzymes: *Sod2* and *-3*, respectively, catalase, *Gpx1*, *-2*, and *-3* respectively; cold/heat-shock induced genes: heat-shock protein -1A and 2A (*Hspa1a* and *-2*, respectively) and heat shock factor 2 (*Hsf2*). Statistical significance at $P < 0.05$ was confirmed with 1-way ANOVA and is shown above the tested column as the number of the CTL column it is paired to.

TABLE 2. *The TRPM8-dependence of gene expression in mouse germ cells subjected to cold shock with a 3 d recovery period*

Markers	Gene	4°C	17°C	29°C
Germ cell types	*Magea4*	1.09	1.49	0.95
	Hspa2	0.88	1.05	0.64
	Tnp1	1.53	1.81	0.81
	Prm2	1.73	1.91	0.76
Cell cycle	*Mki67*	0.89	0.95	0.72
	Pcna	1.38	1.04	0.92
	Cdkn1a	0.65	1.14	0.81
	Cdkn1b	1.32	1.04	0.82
Cell signaling	*Mtor*	0.9	1.06	0.8
	Sp1	1.37	1.61	1.61
ER stress	*Ddit3*	1.57	1.28	0.83
	Atf4	1.62	1.26	0.67
	Eif2ak3	1.14	1.13	0.98
	Sigmar1	1.47	1.17	0.67
Cold/heat shock proteins	*Hsf1*	2.18[a]	1.34	0.89
	Hsf2	0.75	0.75	1.05
	Cirbp	2.16[a]	1.51	1.68
	Hspa1	0.47[b]	0.68	1.08
	Hspa2	0.88	1.05	0.64
	Rbm3	2.11	1.5	0.87
Mitochondrial uncoupling	*Ucp1*	—	—	—
	Ucp2	1.07	1.01	0.78
	Ucp3	2.98[a]	1.56	1.20
Oxidation	*Sod1*	2.08[a]	2.04	1.20
	Sod2	1.12	1.28	0.72
	Sod3	0.75	0.95	0.65
	Cat	1.10	1.37	1.04
	Gpx1	1.62	1.25	0.87
	Gpx2	2.01[a]	1.87	0.94
	Gpx3	1.22	1.06	0.68
	Gpx4	1.71[a]	3.47[a]	3.38[a]
	Gpx5	3.58[a]	1.14	0.52

TRPM8-mediated fold induction of gene expression. Values represent the ratio of averaged gene expression obtained by dividing CTL value by KOM8 value. Statistical analysis was achieved with 1-way ANOVA. [a]TRPM8-dependent induction. [b]TRPM8-dependent repression.

acute cold shocks (8°C and 20°C, respectively, *vs.* 32°C), to characterize the immediate cold-stimulated TRPM8-dependent responsive genes.

Cold transduction via *TRPM8 induced immediate up-regulation of* Gpx4 *and* Gpx5 *concomitantly to an increase in [ROS] in mouse germ cells*

By means of qPCR, to demonstrate the germ cell enrichment of the extracts, we normalized the expression of several germ cell markers in isolated germ cells extract by their expression level in whole testis extracts. A 100-fold increase in the expression of melanoma antigen family A4 (*Magea4*) (marker of spermatogonium) and transition protein 1 (*Tnp1*) and *Prm2* (markers of spermatids) demonstrated the successful enrichment in germ cells in both CTL and KOM8 samples (**Fig. 6*A***). *Trpm8*, *Hspa1a*, *Hsf2*, and *Sod1* were significantly enriched in the germ cell preparation, whereas *Rbm3* was decreased by almost 100 times. Because *Rbm3* is mainly expressed in Sertoli cells (37), this observation confirms the enrichment of our preparations in germ cells.

After exposing isolated germ cells to a cold shock, we performed qPCR fingerprinting of gene expression. A cold-mediated down-regulation of *Hspa2* and *Hsf1* was detected only in KOM8 germ cells, suggesting that TRPM8 expression prevents this cold dependency (**Fig. 6*B***; **Table 3**). Nevertheless, one could also associate this decrease in *Hspa2* expression with a decrease in the proportion of spermatocytes at 20 and 32°C, or to a down-regulation of gene expression. Because CTL and KOM8 germ cells were prepared in similar conditions and because incubations were performed for 1 h, we assumed that the former explanation was unlikely. Besides, the absence of variation of spermatogonium (*Magea4*) and spermatid proportions (*Tnp1* and *Prm2*) confirmed the identical distribution of germ cell subtypes in the different samples. In line with our whole testis analysis (Table 2), we found that both *Gpx4* and *Gpx5* were differentially upregulated by TRPM8 channels in germ cells subjected to a large range of cold temperatures (Fig. 6B; Table 3). In contrast to whole-testis analysis, *Sod1* and *Gpx2* expression were unchanged in germ cells subjected to acute cold, which suggests that, although *Gpx4* and *Gpx5* genes could be directly regulated by acute cold, *Sod1* and *Gpx2* upregulation could result either from their increased expression in other testis cell types, or from a later process taking place during the recovery period. Our results, altogether, suggest that ER TRPM8 channels are cold transducers triggering the expression of detoxifying enzymes in germ cells. Finally, we measured ROS levels to understand why GPX4 and -5 were so quickly and efficiently induced after an acute cold shock in mouse germ cells. Isolated germ cells were loaded with the cytosolic CellRox Deep Red reagent and the nuclear CellRox Green reagent and exposed for 1 h at 8, 20, or 32°C. Fluorescence of ROS reporters was measured by flow cytometry and revealed that the proportion of CTL germ cells showing high [ROS] increased gradually with cooling (Fig. 6*C*). Although the population of KOM8 germ cells with high ROS content did not vary with cold shock, its abundance was about 3 times greater than in CTL cells at 32°C. The cold- and TRPM8-mediated increase in [ROS] correlated with the cold- and TRPM8-dependency of apoptosis induction. This finding emphasizes the relationship between high ROS content and apoptosis, as reported in spermatozoa (14, 15). Furthermore, our results validate the hypothesis that functional TRPM8 channels are necessary in germ cells to modulate [ROS] *via* the upregulation of detoxifying enzymes during mild hypothermia.

DISCUSSION

In this study, mouse germ cells expressed alternate transcripts of the cold and menthol receptor, TRPM8, in addition to the full-length one. TRPM8 activation by menthol triggered Ca^{2+} mobilization from ER stores of germ cells. The increase in [ROS] correlated with the increased rate of apoptosis of meiotic cells after hypothermia. Finally, we showed that TRPM8 channels are required for cold-mediated induction of heat- and cold-shock proteins and of the detoxifying enzymes GPX4 and -5 that in turn protect germ cells from the deleterious effects of ROS.

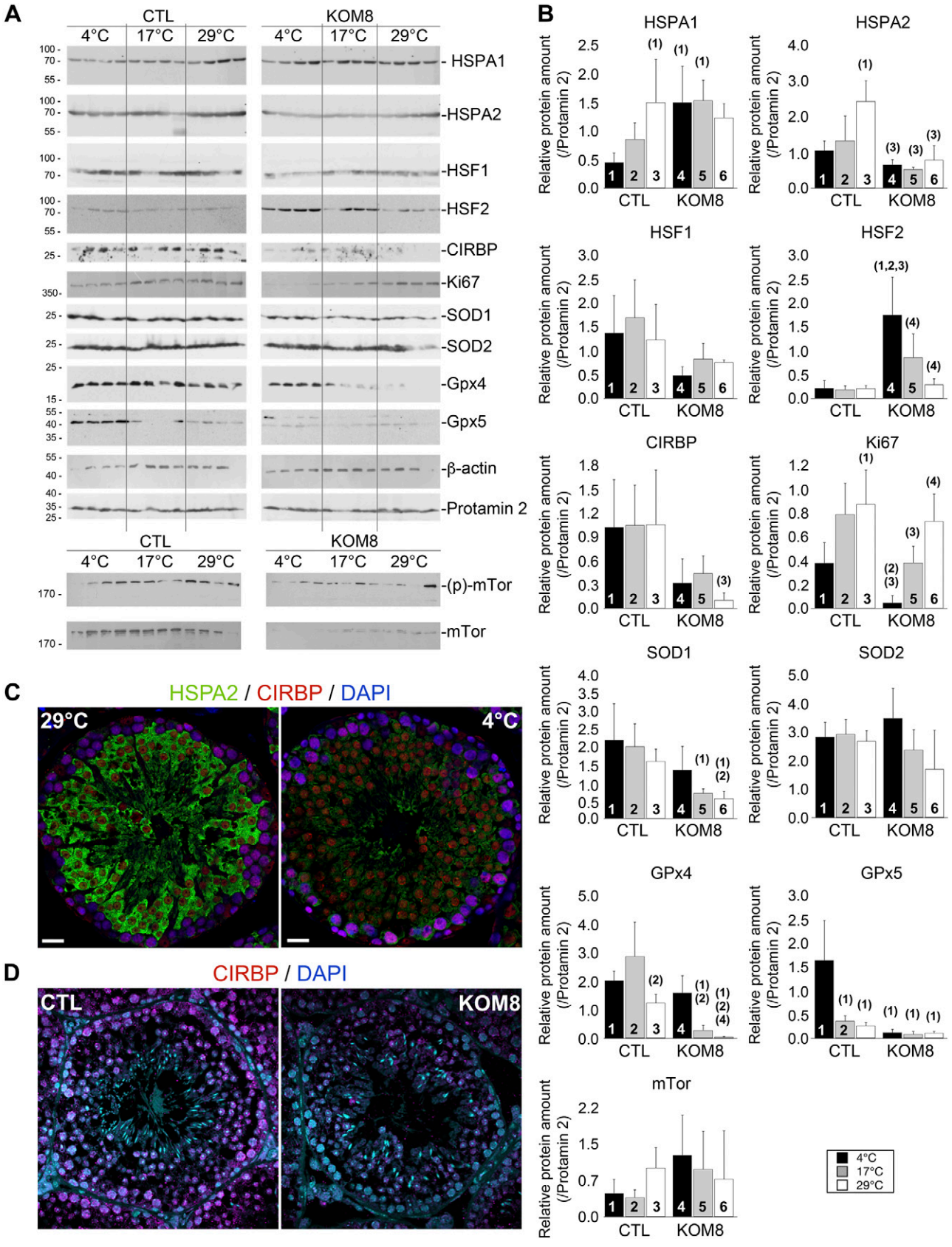

Figure 5. TRPM8 channels participate in the regulation of specific proteins expression in a cold-dependent and cold-independent way. *A*) Immunoblot analysis showing the variation of key protein expression in testis of 4 CTL and 4 KOM8 mice 3 d after cold shock (scrotum temperatures were 29, 17, or 4°C). β-Actin and Prm2 were used as invariant reporters. FKBP-rapamycin–associated protein was detected in its nonphosphorylated and phosphorylated (Ser^{2448}) forms. *B*) Quantification of

(*continued on next page*)

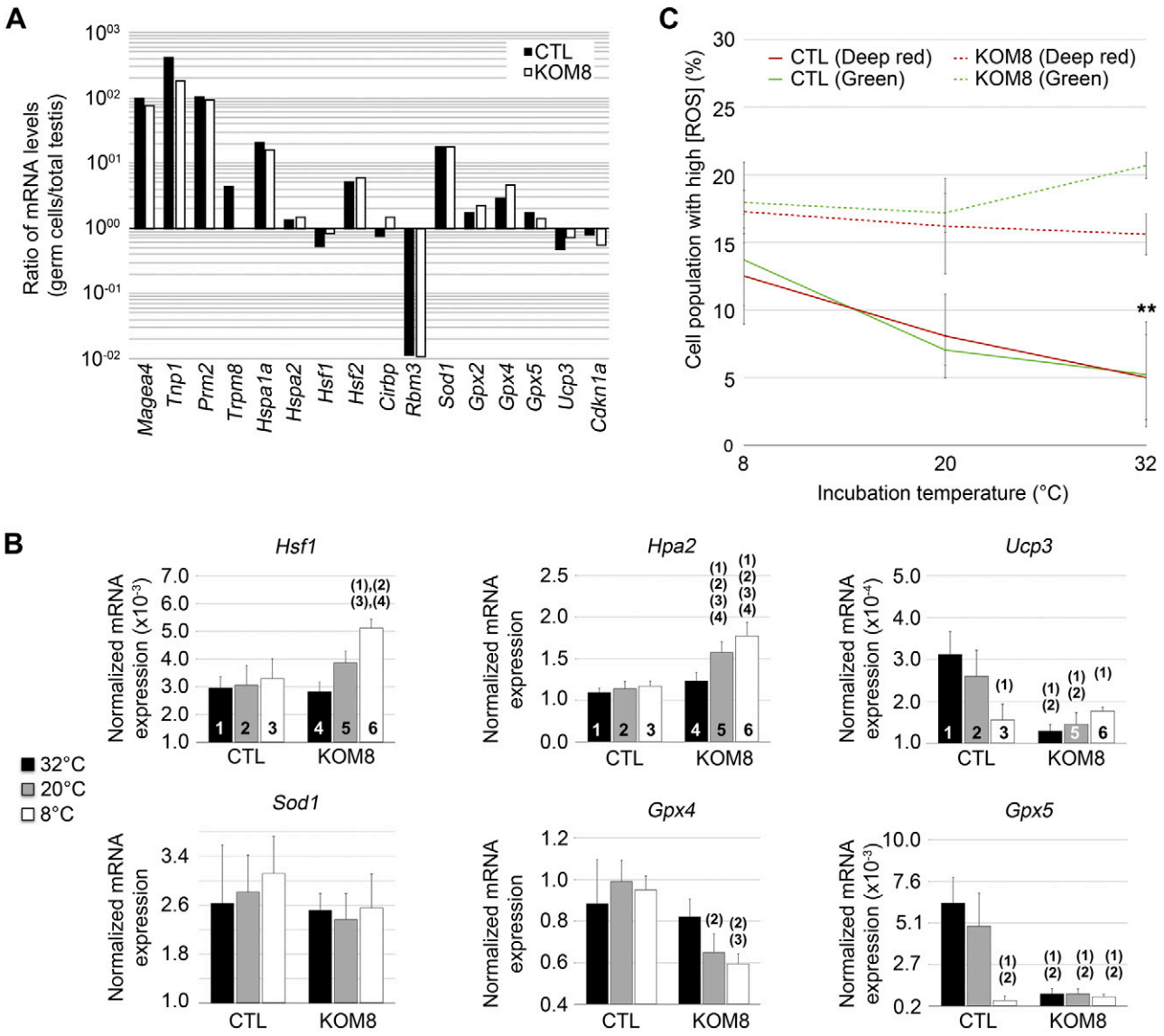

Figure 6. Cold-induced TRPM8 channel activity triggers cold shock response and ROS production. *A*) Expression level of genes of interest in freshly isolated germ cells from either *Trpm8*$^{+/+}$ (CTL; black bars) or *Trpm8*$^{-/-}$ mouse line (KOM8; white bars). Values are expressed as the ratio of gene expression on total mouse testis expression. *Rbm3* was the sole gene with drastically decreased expression in isolated germ cells. Conversely, *Hspa1a*, *Hsf2*, *Sod1*, and *Gpx2* exhibited a preferential expression in germ cells. *B*) Real-time based quantification of mRNA levels of *Hsf1*, *Hspa2*, *Ucp3*, *Sod1*, *Gpx4*, and *Gpx5* in freshly isolated CTL or KOM8 mouse germ cells subjected to a 1-h incubation at 8, 20, or 32°C. Statistical significance (1-way ANOVA) was assumed when $P < 0.05$ and is shown above the tested column as the number of the CTL column it is paired to. *C*) Freshly isolated mouse germ cells were loaded with the nuclear CellROX Green Reagent and the cytosolic/mitochondrial CellROX deep Red Reagent before being subjected to a 1 h cold shock (8°C and 20°C) or kept at CTL temperature (32°C). Cytometer analysis reveals a significant cold-dependent accumulation of ROS in CTL germ cells, whereas stable ROS concentration was observed in KOM8 germ cells. Values are expressed as means ± SD for CTL ($n = 4$) and KOM8 ($n = 4$) mice. Statistical analysis was achieved with a *t* test.

Thermosensitivity of spermatogenesis

In mammals, testes display the unique characteristic of maintaining a lower temperature (32°C) than that of the inner organs. Although the control of scrotum temperature can be partially achieved through body responses, such as adaptation of blood circulation and nutriment availability, thermoshielding mechanisms

the protein levels and statistical significance are reported in (*B*). Protein amount was normalized with Prm2, which appeared much more stable than actin or GAPDH (not shown). Values are presented as means ± SD for CTL ($n = 4$) and KOM8 ($n = 4$) mice. Statistical significance was assumed when $P < 0.05$ and is shown above the tested column as the number of the CTL column it is paired to. *C*, *D*) Immunohistofluorescence confirmed the decreased expression of HSPA2 (*C*, green) in CTL germ cells subjected to hypothermia (*C*, right) compared to CTL (left). CIRBP (red) expression appears stable in both conditions. However, CIRBP was down-regulated in KOM8 testis (*D*, right) when compared to CTL (*D*, left). Nuclei were counterstained with DAPI. Scale bars, 20 μm. Statistical analysis was achieved with 1-way ANOVA.

TABLE 3. *The TRPM8-dependence of gene expression in mouse germ cells subjected to mild or strong cold shocks*

Markers	Gene	8°C	20°C	32°C
Germ cell markers	*mMagea4*	1.23	1.47	1.52
	mTnp1	1.21	1.31	1.53
	mPrm2	1.08	0.82	1.12
Cold/heat shock proteins	*mHSF1*	1.05	0.79	0.64[a]
	mHSF2	0.94	0.97	1.00
	mCIRBP	0.96	1.20	0.89
	mHSPA1	1.14	1.23	1.28
	mHSPA2	0.89	0.72[a]	0.66[a]
Mitochondrial uncoupling	*mUCP3*	2.40[a]	1.78[a]	0.88
Oxidation	*mSOD1*	1.04	1.19	1.22
	mGPX2	1.72	2.23	0.83
	mGPX4	1.08	1.53[a]	1.60[a]
	mGPX5	6.90[b]	5.35[b]	0.73

Data are TRPM8-mediated fold-induction of gene expression. Values represent the ratio of averaged gene expression obtained by dividing CTL value by KOM8 value. Statistical analysis was achieved with 1-way ANOVA. [a]TRPM8-dependent repression. [b]TRPM8-dependent induction.

must be incorporated in germ cells, to guarantee the quickest and the most efficient response to oxidation. Cold shock (<32°C) has been reported to stimulate expression of cold-induced proteins such as CIRBP and RBM3 in numerous tissues (37, 38). It was recently shown that RBM3 protects neurons from ER stress by inhibiting PERK phosphorylation (42). These observations probably explain why both CIRBP and RBM3 are constitutively required in testis. In contrast to cold-shock proteins, HSPs are down-regulated during hypothermia. The HSF family, HSF1, -2, and -4 in mammals, are furthermore sensitive to oxidation, and transduce stress signals to *Hsp* genes. However, variation in ambient temperature is transduced to HSFs. We have shown that steady-state TRPM8 channel activity represses *Hsf1* and *Hspa2* genes at thermoneutrality what probably modify their threshold of activation by heat stress. In the recovery phase after a cold shock, TRPM8 is involved in the repression of *Hspa1* and the induction of *Hsf1*, *Hspa2*, *Cirbp*, and *Rbm3*, which most likely participates in the modulation of ER stress (42). This emphasizes the bimodal regulation of *Hsf1* and *Hspa2* genes after hypothermia.

Amplitude of cold exposure differentially induces ROS-scavenging enzymes in germ cells

The ROS and their derived reactive nitrogen species have been characterized as the main contributors to cell death in hyperthermia (43). In this study, we correlated the cold response to an increase in both [ROS] and apoptosis of spermatocytes. Cooling and heating induce common pathways, including synthesis of chaperones (heat- *vs.* cold-shock proteins), PERK-mediated ER stress (44), and increased activity of GPXs and catalase [in endotherms (45, 46) and ectotherms (47)]. Others have suggested that this increased GPX activity would enhance detoxification of ROS and consequently increase cell survival (14, 15, 48). In our study, we demonstrated the cold-mediated induction of ROS-scavenging enzymes in mammal testis: *Gpx2*, *-4*, and *-5*, and *Sod1*. Although GPX4 and -5 are mainly expressed in the male genital tract, SOD1 and GPX2 are found in all tissues. GPX4 is a selenium-dependent scavenger that metabolizes reactive H_2O_2 and complexes organic peroxidized molecules in H_2O (for review, see ref. 49). Suppression of the mitochondrial GPX4 increases ROS content and triggers infertility (50), demonstrating its critical role in ROS detoxification. GPX5 is a selenium-dependent scavenger that is mainly expressed in epididymis spermatozoa. GPX5 deletion increases ROS content in spermatozoa and decreases viability of resulting embryos (51). Our results demonstrate that TRPM8 sustains GPX4 expression between 17 and 32°C, whereas it upregulates GPX5 at a colder range of temperatures (>20°C). Taking into account that TRPM8 range of activity is between 15 and 32°C, it is noteworthy that GPX4 and -5 are differentially regulated by the same cold-activated TRPM8 response, suggesting that GPX4 and -5 are likely regulated by different pathways or require different levels of TRPM8 activation.

Another regulator of ROS content, which is not an ROS scavenger, *per se*, has recently emerged in the literature. Except in thermogenic tissues, uncoupling has been postulated to participate in ROS homeostasis. Superoxide activates UCP3, which triggers a proton leak, and consequently, uncoupling (52). This, in turn, decreases the rate of production of new superoxide anions, and may help to decrease [ROS] in cells (40, 53). Likewise, hyperthermia stimulates UCP2 expression, which, in turn, increases uncoupling and prevents production of high levels of ROS (54). In our hands, UCP3 regulation by cold is similar to GPX5 and requires functional TRPM8 channels. In contract with GPX4, UCP3 and GPX5 expression levels fit well with the proportion of CTL germ cells characterized by a high ROS content. This result suggests that at basal temperature, GPX4 is the main ROS scavenger active in germ cells, whereas, during mild hypothermia, both GPX5 and UCP3 are activated *via* TRPM8 sensors, to enhance ROS scavenging.

Altogether, these mechanisms confer on rodent germ cells graduated responses to cold-mediated ROS induction that efficiently protect them from cell death during hypothermia ranging from 17 to 30°C. However, acute cold (<15°C) probably triggers more effects that cannot be completely prevented by the triad TRPM8/GPX4/GPX5.

TRPM8/Ca^{2+}/ROS, the triad regulating cold-induced apoptosis in germ cells

Increasing evidence characterized ROS as crucial second messengers inducing cell death (55). This function implies that ROS homeostasis must be finely tuned to control the [ROS] and thus prevent cell death in the absence of catastrophic stimulation (56). At scrotum physiologic temperatures, TRPM8 expression exerts a protective effect by indirectly up-regulating GPX4 levels. This finding likely explains why ROS content is lower in CTL germ cells than in KOM8 cells. Although the steady-state thermo-dependent TRPM8 activity is probably negligible at

32°C, the channel can still be activated by lipids (57, 58). TRPM8 activation by cold clearly induces GPX5/UCP3 expression, likely to prevent an adverse increase in ROS content. We recently showed that a similar isoform of TRPM8 induces Ca^{2+} shuttling from ER microdomains to mitochondria in keratinocytes. This phenomenon is followed by boosts in trichloroacetic activity and the associated superoxide production (10). Therefore, it is likely that cold stimulation of germ cells stimulates ROS production through a Ca^{2+}-dependent TRPM8-mediated mechanism. Along this line, a Ca^{2+}-dependent Src and Ras/cAMP pathway induces Gpx1 expression in yeast (59), and a Ca^{2+}-dependent calcineurin/crz-1 pathway induces Gpx2 expression (60). Therefore, we cannot exclude that Ca^{2+} leaking from TRPM8 channels could stimulate both *Gpx4* and *-5* genes. In summary, the TRPM8 channel most likely participates in the modulation of antioxidant factors and thus in the redox homeostasis *via* both calcium and ROS signals. FJ

The authors thank the whole Genoway team and Charles River Laboratories (Lyon, France) for their support and their expertise; and Delphine Taillieu and Mélanie Besegher for technical assistance in animal housing at Animalerie High-Tech de l'Institut de Médecine Prédictive et de Recherche Thérapeutique de Lille. The *Trpm8*$^{-/-}$ mouse line was designed by G.B. and Genoway Inc. The *Trpm8*$^{-/-}$ mouse line was established by Genoway Inc. and housed at Charles River Laboratories. This work was supported by grants from INSERM, Ministère de l'Education Nationale, Ligue Nationale Contre le Cancer, Region Nord-Pas-de-Calais, and ANR Grant TRPM8/REPROD. A.-S.B. was supported by Fondation pour la recherche médicale. Author Contributions: A.-S. Borowiec and G. Bidaux designed research; A.-S. Borowiec, B. Sion, F. Chalmel, A. D. Rolland, L. Lemonnier, T. De Clerck, A. Bokhobza, S. Derouiche, E. Dewailly, C. Slomianny, C. Mauduit, and G. Bidaux performed research; A.-S. Borowiec, B. Sion, F. Chalmel, A. D. Rolland, L. Lemonnier, C. Slomianny, M. Benahmed, M. Roudbaraki, B. Jégou, and G. Bidaux analyzed data; and A.-S. Borowiec, B. Sion, F. Chalmel, A. D. Rolland, L. Lemonnier, B. Jégou, N. Prevarskaya, and G. Bidaux wrote the paper. The authors declare no conflicts of interest.

REFERENCES

1. Chowdhury, A. K., and Steinberger, E. (1970) Early changes in the germinal epithelium of rat testes following exposure to heat. *J. Reprod. Fertil.* **22**, 205–212
2. Macdonald, J., and Harrison, R. G. (1954) Effect of low temperatures on rat spermatogenesis. *Fertil. Steril.* **5**, 205–216
3. Blanco-Rodríguez, J., and Martínez-García, C. (1997) Mild hypothermia induces apoptosis in rat testis at specific stages of the seminiferous epithelium. *J. Androl.* **18**, 535–539
4. Zhang, Z., Short, R. V., Meehan, T., De Kretser, D. M., Renfree, M. B., and Loveland, K. L. (2004) Functional analysis of the cooled rat testis. *J. Androl.* **25**, 57–68
5. Yazawa, T., Nakayama, Y., Fujimoto, K., Matsuda, Y., Abe, K., Kitano, T., Abé, S., and Yamamoto, T. (2003) Abnormal spermatogenesis at low temperatures in the Japanese red-bellied newt, Cynops pyrrhogaster: possible biological significance of the cessation of spermatocytogenesis. *Mol. Reprod. Dev.* **66**, 60–66
6. Brauchi, S., Orio, P., and Latorre, R. (2004) Clues to understanding cold sensation: thermodynamics and electrophysiological analysis of the cold receptor TRPM8. *Proc. Natl. Acad. Sci. USA* **101**, 15494–15499
7. Voets, T., Droogmans, G., Wissenbach, U., Janssens, A., Flockerzi, V., and Nilius, B. (2004) The principle of temperature-dependent gating in cold- and heat-sensitive TRP channels. *Nature* **430**, 748–754
8. Bidaux, G., Flourakis, M., Thebault, S., Zholos, A., Beck, B., Gkika, D., Roudbaraki, M., Bonnal, J. L., Mauroy, B., Shuba, Y., Skryma, R., and Prevarskaya, N. (2007) Prostate cell differentiation status determines transient receptor potential melastatin member 8 channel subcellular localization and function. *J. Clin. Invest.* **117**, 1647–1657
9. Denda, M., Tsutsumi, M., and Denda, S. (2010) Topical application of TRPM8 agonists accelerates skin permeability barrier recovery and reduces epidermal proliferation induced by barrier insult: role of cold-sensitive TRP receptors in epidermal permeability barrier homoeostasis. *Exp. Dermatol.* **19**, 791–795
10. Bidaux, G., Borowiec, A. S., Gordienko, D., Beck, B., Shapovalov, G. G., Lemonnier, L., Flourakis, M., Vandenberghe, M., Slomianny, C., Dewailly, E., Delcourt, P., Desruelles, E., Ritaine, A., Polakowska, R., Lesage, J., Chami, M., Skryma, R., and Prevarskaya, N. (2015) Epidermal TRPM8 channel isoform controls the balance between keratinocyte proliferation and differentiation in a cold-dependent manner. *Proc. Natl. Acad. Sci. USA* **112**, E3345–E3354
11. Bidaux, G., Borowiec, A. S., Prevarskaya, N., and Gordienko, D. (2016) Fine-tuning of eTRPM8 expression and activity conditions keratinocyte fate. [E-pub ahead of print]. *Channels (Austin)* doi:10.1080/19336950.2016.1168551
12. Nocchi, L., Daly, D. M., Chapple, C., and Grundy, D. (2014) Induction of oxidative stress causes functional alterations in mouse urothelium via a TRPM8-mediated mechanism: implications for aging. *Aging Cell* **13**, 540–550
13. Zhu, S., Wang, Y., Pan, L., Yang, S., Sun, Y., Wang, X., and Hu, F. (2014) Involvement of transient receptor potential melastatin-8 (TRPM8) in menthol-induced calcium entry, reactive oxygen species production and cell death in rheumatoid arthritis rat synovial fibroblasts. *Eur. J. Pharmacol.* **725**, 1–9
14. Aitken, R. J., and Baker, M. A. (2013) Causes and consequences of apoptosis in spermatozoa; contributions to infertility and impacts on development. *Int. J. Dev. Biol.* **57**, 265–272
15. Aitken, R. J., Whiting, S., De Iuliis, G. N., McClymont, S., Mitchell, L. A., and Baker, M. A. (2012) Electrophilic aldehydes generated by sperm metabolism activate mitochondrial reactive oxygen species generation and apoptosis by targeting succinate dehydrogenase. *J. Biol. Chem.* **287**, 33048–33060
16. De Blas, G. A., Darszon, A., Ocampo, A. Y., Serrano, C. J., Castellano, L. E., Hernández-González, E. O., Chirinos, M., Larrea, F., Beltrán, C., and Treviño, C. L. (2009) TRPM8, a versatile channel in human sperm. *PLoS One* **4**, e6095
17. Gibbs, G. M., Orta, G., Reddy, T., Koppers, A. J., Martínez-López, P., de la Vega-Beltràn, J. L., Lo, J. C., Veldhuis, N., Jamsai, D., McIntyre, P., Darszon, A., and O'Bryan, M. K. (2011) Cysteine-rich secretory protein 4 is an inhibitor of transient receptor potential M8 with a role in establishing sperm function. *Proc. Natl. Acad. Sci. USA* **108**, 7034–7039
18. Martínez-López, P., Treviño, C. L., de la Vega-Beltrán, J. L., De Blas, G., Monroy, E., Beltrán, C., Orta, G., Gibbs, G. M., O'Bryan, M. K., and Darszon, A. (2011) TRPM8 in mouse sperm detects temperature changes and may influence the acrosome reaction. *J. Cell. Physiol.* **226**, 1620–1631
19. World Health Organization. (2001) Laboratory manual of the WHO for the examination of human semen and sperm-cervical mucus interaction [in Italian]. *Ann. Ist. Super. Sanita* **37**, I–XII, 1–123
20. Chalmel, F., Rolland, A. D., Niederhauser-Wiederkehr, C., Chung, S. S., Demougin, P., Gattiker, A., Moore, J., Patard, J. J., Wolgemuth, D. J., Jégou, B., and Primig, M. (2007) The conserved transcriptome in human and rodent male gametogenesis. *Proc. Natl. Acad. Sci. USA* **104**, 8346–8351
21. Gan, H., Wen, L., Liao, S., Lin, X., Ma, T., Liu, J., Song, C. X., Wang, M., He, C., Han, C., and Tang, F. (2013) Dynamics of 5-hydroxymethylcytosine during mouse spermatogenesis. *Nat. Commun.* **4**, 1995
22. Soumillon, M., Necsulea, A., Weier, M., Brawand, D., Zhang, X., Gu, H., Barthès, P., Kokkinaki, M., Nef, S., Gnirke, A., Dym, M., de Massy, B., Mikkelsen, T. S., and Kaessmann, H. (2013) Cellular source and mechanisms of high transcriptome complexity in the mammalian testis. *Cell Reports* **3**, 2179–2190
23. Darde, T. A., Sallou, O., Becker, E., Evrard, B., Monjeaud, C., Le Bras, Y., Jégou, B., Collin, O., Rolland, A. D., and Chalmel, F. (2015) The ReproGenomics Viewer: an integrative cross-species toolbox for the reproductive science community. *Nucleic Acids Res.* **43**(W1), W109–W116
24. Schultz, N., Hamra, F. K., and Garbers, D. L. (2003) A multitude of genes expressed solely in meiotic or postmeiotic spermatogenic cells offers a myriad of contraceptive targets. *Proc. Natl. Acad. Sci. USA* **100**, 12201–12206

25. Shima, J. E., McLean, D. J., McCarrey, J. R., and Griswold, M. D. (2004) The murine testicular transcriptome: characterizing gene expression in the testis during the progression of spermatogenesis. *Biol. Reprod.* **71**, 319–330
26. Namekawa, S. H., Park, P. J., Zhang, L. F., Shima, J. E., McCarrey, J. R., Griswold, M. D., and Lee, J. T. (2006) Postmeiotic sex chromatin in the male germline of mice. *Curr. Biol.* **16**, 660–667
27. Irizarry, R. A., Bolstad, B. M., Collin, F., Cope, L. M., Hobbs, B., and Speed, T. P. (2003) Summaries of Affymetrix GeneChip probe level data. *Nucleic Acids Res.* **31**, e15
28. Chalmel, F., and Primig, M. (2008) The Annotation, Mapping, Expression and Network (AMEN) suite of tools for molecular systems biology. *BMC Bioinformatics* **9**, 86
29. Lardenois, A., Gattiker, A., Collin, O., Chalmel, F., and Primig, M. (2010) GermOnline 4.0 is a genomics gateway for germline development, meiosis and the mitotic cell cycle. *Database (Oxford)* **2010**, baq030
30. Bidaux, G., Roudbaraki, M., Merle, C., Crépin, A., Delcourt, P., Slomianny, C., Thebault, S., Bonnal, J. L., Benahmed, M., Cabon, F., Mauroy, B., and Prevarskaya, N. (2005) Evidence for specific TRPM8 expression in human prostate secretory epithelial cells: functional androgen receptor requirement. *Endocr. Relat. Cancer* **12**, 367–382
31. Vandesompele, J., De Preter, K., Pattyn, F., Poppe, B., Van Roy, N., De Paepe, A., and Speleman, F. (2002) Accurate normalization of real-time quantitative RT-PCR data by geometric averaging of multiple internal control genes. *Genome Biol.* 3, RESEARCH0034
32. Thebault, S., Lemonnier, L., Bidaux, G., Flourakis, M., Bavencoffe, A., Gordienko, D., Roudbaraki, M., Delcourt, P., Panchin, Y., Shuba, Y., Skryma, R., and Prevarskaya, N. (2005) Novel role of cold/menthol-sensitive transient receptor potential melastatine family member 8 (TRPM8) in the activation of store-operated channels in LNCaP human prostate cancer epithelial cells. *J. Biol. Chem.* **280**, 39423–39435
33. Grynkiewicz, G., Poenie, M., and Tsien, R. Y. (1985) A new generation of Ca2+ indicators with greatly improved fluorescence properties. *J. Biol. Chem.* **260**, 3440–3450
34. Brauchi, S., Orta, G., Salazar, M., Rosenmann, E., and Latorre, R. (2006) A hot-sensing cold receptor: C-terminal domain determines thermosensation in transient receptor potential channels. *J. Neurosci.* **26**, 4835–4840
35. McKemy, D. D., Neuhausser, W. M., and Julius, D. (2002) Identification of a cold receptor reveals a general role for TRP channels in thermosensation. *Nature* **416**, 52–58
36. Peier, A. M., Moqrich, A., Hergarden, A. C., Reeve, A. J., Andersson, D. A., Story, G. M., Earley, T. J., Dragoni, I., McIntyre, P., Bevan, S., and Patapoutian, A. (2002) A TRP channel that senses cold stimuli and menthol. *Cell* **108**, 705–715
37. Danno, S., Itoh, K., Matsuda, T., and Fujita, J. (2000) Decreased expression of mouse Rbm3, a cold-shock protein, in Sertoli cells of cryptorchid testis. *Am. J. Pathol.* **156**, 1685–1692
38. Nishiyama, H., Itoh, K., Kaneko, Y., Kishishita, M., Yoshida, O., and Fujita, J. (1997) A glycine-rich RNA-binding protein mediating cold-inducible suppression of mammalian cell growth. *J. Cell Biol.* **137**, 899–908
39. Wang, X., Sharma, R. K., Sikka, S. C., Thomas, A. J., Jr., Falcone, T., and Agarwal, A. (2003) Oxidative stress is associated with increased apoptosis leading to spermatozoa DNA damage in patients with male factor infertility. *Fertil. Steril.* **80**, 531–535
40. Liu, D., Huang, L., Wang, Y., Wang, W., Wehrens, X. H., Belousova, T., Abdelrahim, M., DiMattia, G., and Sheikh-Hamad, D. (2012) Human stanniocalcin-1 suppresses angiotensin II-induced superoxide generation in cardiomyocytes through UCP3-mediated anti-oxidant pathway. *PLoS One* **7**, e36994
41. Hofmann, S., Cherkasova, V., Bankhead, P., Bukau, B., and Stoecklin, G. (2012) Translation suppression promotes stress granule formation and cell survival in response to cold shock. *Mol. Biol. Cell* **23**, 3786–3800
42. Zhu, X., Zelmer, A., Kapfhammer, J. P., and Wellmann, S. (2016) Cold-inducible RBM3 inhibits PERK phosphorylation through cooperation with NF90 to protect cells from endoplasmic reticulum stress. *FASEB J.* 30, 624–634
43. Pino, J. A., Osses, N., Oyarzún, D., Farías, J. G., Moreno, R. D., and Reyes, J. G. (2013) Differential effects of temperature on reactive oxygen/nitrogen species production in rat pachytene spermatocytes and round spermatids. *Reproduction* **145**, 203–212
44. Avivar-Valderas, A., Salas, E., Bobrovnikova-Marjon, E., Diehl, J. A., Nagi, C., Debnath, J., and Aguirre-Ghiso, J. A. (2011) PERK integrates autophagy and oxidative stress responses to promote survival during extracellular matrix detachment. *Mol. Cell. Biol.* **31**, 3616–3629
45. Kaushik, S., and Kaur, J. (2003) Chronic cold exposure affects the antioxidant defense system in various rat tissues. *Clin. Chim. Acta* 333, 69–77
46. Selman, C., McLaren, J. S., Himanka, M. J., and Speakman, J. R. (2000) Effect of long-term cold exposure on antioxidant enzyme activities in a small mammal. *Free Radic. Biol. Med.* **28**, 1279–1285
47. Voituron, Y., Servais, S., Romestaing, C., Douki, T., and Barré, H. (2006) Oxidative DNA damage and antioxidant defenses in the European common lizard (Lacerta vivipara) in supercooled and frozen states. *Cryobiology* **52**, 74–82
48. Ishii, T., Matsuki, S., Iuchi, Y., Okada, F., Toyosaki, S., Tomita, Y., Ikeda, Y., and Fujii, J. (2005) Accelerated impairment of spermatogenic cells in SOD1-knockout mice under heat stress. *Free Radic. Res.* **39**, 697–705
49. Chabory, E., Damon, C., Lenoir, A., Henry-Berger, J., Vernet, P., Cadet, R., Saez, F., and Drevet, J. R. (2010) Mammalian glutathione peroxidases control acquisition and maintenance of spermatozoa integrity. *J. Anim. Sci.* **88**, 1321–1331
50. Schneider, M., Förster, H., Boersma, A., Seiler, A., Wehnes, H., Sinowatz, F., Neumüller, C., Deutsch, M. J., Walch, A., Hrabé de Angelis, M., Wurst, W., Ursini, F., Roveri, A., Maleszewski, M., Maiorino, M., and Conrad, M. (2009) Mitochondrial glutathione peroxidase 4 disruption causes male infertility. *FASEB J.* **23**, 3233–3242
51. Chabory, E., Damon, C., Lenoir, A., Kauselmann, G., Kern, H., Zevnik, B., Garrel, C., Saez, F., Cadet, R., Henry-Berger, J., Schoor, M., Gottwald, U., Habenicht, U., Drevet, J. R., and Vernet, P. (2009) Epididymis seleno-independent glutathione peroxidase 5 maintains sperm DNA integrity in mice. *J. Clin. Invest.* **119**, 2074–2085
52. Papa, S., and Skulachev, V. P. (1997) Reactive oxygen species, mitochondria, apoptosis and aging. *Mol. Cell. Biochem.* **174**, 305–319
53. Echtay, K. S., Roussel, D., St-Pierre, J., Jekabsons, M. B., Cadenas, S., Stuart, J. A., Harper, J. A., Roebuck, S. J., Morrison, A., Pickering, S., Clapham, J. C., and Brand, M. D. (2002) Superoxide activates mitochondrial uncoupling proteins. *Nature* **415**, 96–99
54. Zhang, K., Shang, Y., Liao, S., Zhang, W., Nian, H., Liu, Y., Chen, Q., and Han, C. (2007) Uncoupling protein 2 protects testicular germ cells from hyperthermia-induced apoptosis. *Biochem. Biophys. Res. Commun.* **360**, 327–332
55. Imai, H., and Nakagawa, Y. (2003) Biological significance of phospholipid hydroperoxide glutathione peroxidase (PHGPx, GPx4) in mammalian cells. *Free Radic. Biol. Med.* **34**, 145–169
56. Ray, P. D., Huang, B. W., and Tsuji, Y. (2012) Reactive oxygen species (ROS) homeostasis and redox regulation in cellular signaling. *Cell. Signal.* **24**, 981–990
57. Vanden Abeele, F., Zholos, A., Bidaux, G., Shuba, Y., Thebault, S., Beck, B., Flourakis, M., Panchin, Y., Skryma, R., and Prevarskaya, N. (2006) Ca^{2+}-independent phospholipase A2-dependent gating of TRPM8 by lysophospholipids. *J. Biol. Chem.* **281**, 40174–40182
58. Andersson, D. A., Nash, M., and Bevan, S. (2007) Modulation of the cold-activated channel TRPM8 by lysophospholipids and polyunsaturated fatty acids. *J. Neurosci.* **27**, 3347–3355
59. Ohdate, T., Izawa, S., Kita, K., and Inoue, Y. (2010) Regulatory mechanism for expression of GPX1 in response to glucose starvation and Ca in Saccharomyces cerevisiae: involvement of Snf1 and Ras/cAMP pathway in Ca signaling. *Genes Cells* 15, 59–75
60. Tsuzi, D., Maeta, K., Takatsume, Y., Izawa, S., and Inoue, Y. (2004) Distinct regulatory mechanism of yeast GPX2 encoding phospholipid hydroperoxide glutathione peroxidase by oxidative stress and a calcineurin/Crz1-mediated Ca^{2+} signaling pathway. *FEBS Lett.* **569**, 301–306

Received for publication February 16, 2016.
Accepted for publication May 23, 2016.

Cold/menthol TRPM8 receptors initiate the cold-shock response and protect germ cells from cold-shock –induced oxidation

Anne-Sophie Borowiec, Benoit Sion, Frédéric Chalmel, et al.

FASEB J 2016 30: 3155-3170 originally published online June 17, 2016
Access the most recent version at doi:10.1096/fj.201600257R